

## NEW RESEARCH PAPER

# Association of Regional Wall Shear Stress and Progressive Ascending Aorta Dilation in Bicuspid Aortic Valve

Gilles Soulat, MD, PhD,<sup>a,\*</sup> Michael B. Scott, PhD,<sup>a,b,\*</sup> Bradley D. Allen, MD,<sup>a</sup> Ryan Avery, MD,<sup>a</sup> Robert O. Bonow, MD,<sup>c</sup> S. Chris Malaisrie, MD,<sup>d</sup> Patrick McCarthy, MD,<sup>d</sup> Paul W.M. Fedak, MD, PhD,<sup>d,e</sup> Alex J. Barker, PhD,<sup>f</sup> Michael Markl, PhD<sup>a,b</sup>

## ABSTRACT

**OBJECTIVES** The aim of this study was to evaluate the role of wall shear stress (WSS) as a predictor of ascending aorta (AAo) growth at 5 years or greater follow-up.

**BACKGROUND** Aortic 4-dimensional flow cardiac magnetic resonance (CMR) can quantify regions exposed to high WSS, a known stimulus for arterial wall dysfunction. However, its association with longitudinal changes in aortic dilation in patients with bicuspid aortic valve (BAV) is unknown.

**METHODS** This retrospective study identified 72 patients with BAV ( $45 \pm 12$  years) who underwent CMR for surveillance of aortic dilation at baseline and  $\geq 5$  years of follow-up. Four-dimensional flow CMR analysis included the calculation of WSS heat maps to compare regional WSS in individual patients with population averages of healthy age- and sex-matched subjects (database of 136 controls). The relative areas of the AAo and aorta (in %) exposed to elevated WSS (outside the 95% CI of healthy population averages) were quantified.

**RESULTS** At a median follow-up duration of 6.0 years, the mean AAo growth rate was  $0.24 \pm 0.20$  mm/y. The fraction of the AAo exposed to elevated WSS at baseline was increased for patients with higher growth rates ( $>0.24$  mm/y,  $n = 32$ ) compared with those with growth rates  $<0.24$  mm/y (19.9% [interquartile range (IQR): 10.2-25.5] vs 5.7% [IQR: 1.5-21.3];  $P = 0.008$ ). Larger areas of elevated WSS in the AAo and entire aorta were associated with higher rates of AAo dilation  $>0.24$  mm/y (odds ratio: 1.51; 95% CI: 1.05-2.17;  $P = 0.026$  and odds ratio: 1.70; 95% CI: 1.01-3.15;  $P = 0.046$ , respectively).

**CONCLUSIONS** The area of elevated AAo WSS as assessed by 4-dimensional flow CMR identified BAV patients with higher rates of aortic dilation and thus might determine which patients require closer follow-up.

(J Am Coll Cardiol Img 2021;■:■-■) © 2021 by the American College of Cardiology Foundation.

From the <sup>a</sup>Department of Radiology, Feinberg School of Medicine, Northwestern University, Chicago, Illinois, USA; <sup>b</sup>Department of Biomedical Engineering, McCormick School of Engineering, Northwestern University, Evanston, Illinois, USA; <sup>c</sup>Division of Cardiology, Department of Medicine, Bluhm Cardiovascular Institute, Northwestern University, Chicago, Illinois, USA; <sup>d</sup>Division of Cardiac Surgery, Department of Surgery, Bluhm Cardiovascular Institute, Northwestern University, Chicago, Illinois, USA; <sup>e</sup>Department of Cardiac Sciences, Section of Cardiac Surgery Cumming School of Medicine, University of Calgary, Libin Cardiovascular Institute, Calgary, Alberta, Canada; and the <sup>f</sup>Department of Radiology and Bioengineering, Anschutz Medical Campus, University of Colorado, Aurora, Colorado, USA. \*Drs Soulat and Scott contributed equally to this work and are co-first authors.

The authors attest they are in compliance with human studies committees and animal welfare regulations of the authors' institutions and Food and Drug Administration guidelines, including patient consent where appropriate. For more information, visit the [Author Center](#).

Manuscript received April 5, 2021; revised manuscript received June 2, 2021, accepted June 7, 2021.

## ABBREVIATIONS AND ACRONYMS

**AAo** = ascending aorta

**BAV** = bicuspid aortic valve

**BMI** = body mass index

**BSA** = body surface area

**CMR** = cardiac magnetic resonance

**IQR** = interquartile range

**MRA** = magnetic resonance angiography

**OR** = odds ratio

**SSFP** = steady-state free precession

**WSS** = wall shear stress

Progressive aortic dilation is associated with severe complications such as ascending aorta (AAo) aneurysm, dissection, and rupture. Recent guidelines recommend preventive surgery for AAo dilation depending on aortic dimensions, etiology, and comorbidities or in patients with high growth rates ( $>3$  mm/y) (1,2). However, independent predictors of AAo growth rate to identify patients at highest risk of progressive aortic dilation and secondary complications are largely unknown (2). In patients with congenitally abnormal bicuspid aortic valves (BAVs), prior studies have identified the phenotype of the aortic dilation pattern as a risk factor for progression (3,4), but the

data remain heterogeneous and are not used for patient management (1,2,5,6).

In the past decade, 4-dimensional (4D) flow cardiac magnetic resonance (CMR) has emerged as a versatile technique for in vivo measurement of aortic 3-dimensional (3D) hemodynamics and their interactions with the vessel wall (7-9). Aortic 4D flow CMR can quantify AAo regions exposed to high wall shear stress (WSS), a known stimulus for vessel wall remodeling related with arterial medial wall degeneration (10,11). To account for well-known changes in aortic flow and WSS with age and sex (12-14), the concept of a "WSS heat map" has recently been developed in which areas of elevated WSS are identified by comparing the aortic WSS distribution in an individual patient with CIs and population averages of WSS in healthy age- and sex-matched control cohorts (15,16). Areas of elevated WSS have been associated with AAo medial wall degeneration in histopathologic examination in BAV patients (11,17), making WSS a promising metric to predict aortic complications.

However, the relationship between the areas of elevated WSS and aortic growth rates in BAV aortopathy has not been established because of a lack of long-term 4D flow follow-up data and the slow growth rates of the aorta (3,4). The aim of this study was to evaluate the diagnostic value of 4D flow metrics, including WSS, as predictors of AAo growth in BAV patients over more than 5 years of follow-up.

## METHODS

An institutional 4D flow CMR database consisting of 1,061 4D flow CMR baseline examinations from adult BAV patients was queried for patients who underwent CMR between April 1, 2011, and October 31, 2020. This database contains BAV patients who

underwent standard of care CMR for aortic dilation and/or aortic valve disease including aortic 4D flow CMR. The inclusion criteria were BAV and baseline cardiothoracic CMR (including aortic 4D flow CMR) with another CMR examination at  $\geq 5$  years of follow-up. The exclusion criteria were known connective tissue disease or aortic or valve surgery before the follow-up CMR examination. A total of 117 BAV patients with baseline and follow-up cardiothoracic CMR were retrospectively identified. To evaluate the natural progression of the disease, 35 patients who underwent aortic or valve surgery before or between the CMR examinations were excluded (including 4 with childhood repair of aortic coarctation), and 10 patients were excluded because of missing data related to incomplete data transfer. No patients meeting the inclusion criteria had known connective tissue disease. Thus, a total of 72 patients (mean age  $45 \pm 12$  years, 50 men) were included in the final analysis.

Healthy controls ( $n = 136$ , age range 19 years-81 years, 67 men, 69 women) with no known cardiovascular disease and a normal functioning tricuspid aortic valve were included as part of an ongoing institutional review board-approved study in order to compute regionally resolved 95% CI values for physiologically normal aortic WSS.

Informed consent was prospectively obtained from all controls. All patients undergoing standard of care CMR were enrolled by retrospective chart review and waiver of consent. All subjects were included in the study according to procedures approved by the Northwestern University Institutional Review Board.

**CARDIOTHORACIC CMR.** All patients and controls underwent cardiothoracic CMR on a 1.5-T or 3-T CMR system (MAGNETOM Aera, Avanto, Skyra, Siemens Healthcare). The left ventricle was covered using a stack of cine steady-state free precession (SSFP) sequences according to the Society for Cardiovascular Magnetic Resonance guidelines (18). For patients, an aortic angiogram was acquired using either 3D contrast-enhanced magnetic resonance angiography (MRA) (spatial resolution =  $0.6\text{-}1.2 \times 0.6\text{-}1.2 \times 1.0\text{-}2.0$  mm<sup>3</sup>, flip angle =  $25^\circ\text{-}40^\circ$ ) after injection of a chelated gadolinium contrast agent (Ablavar [Lantheus Medical Imaging], Gadavist [Bayer Healthcare], Magnevist [Bayer Healthcare], or Multihance [Bracco Diagnostics]) or a 3D cardiac gated SSFP in free breathing with a diaphragm navigator (spatial resolution =  $0.7\text{-}1.5 \times 0.7\text{-}1.5 \times 1.2\text{-}2.0$  mm<sup>3</sup>, flip angle =  $18^\circ\text{-}70^\circ$ ).

Two-dimensional (2D) cine phase-contrast CMR was also acquired in patients at the sinotubular junction, perpendicular to the centerline of the aorta

(spatial resolution =  $1.7\text{--}2.0 \times 1.7\text{--}2.0 \times 6.0 \text{ mm}^3$ , temporal resolution = 31 milliseconds-71 milliseconds, flip angle =  $20^\circ\text{--}30^\circ$ , velocity sensitivity = 110-400 cm/s).

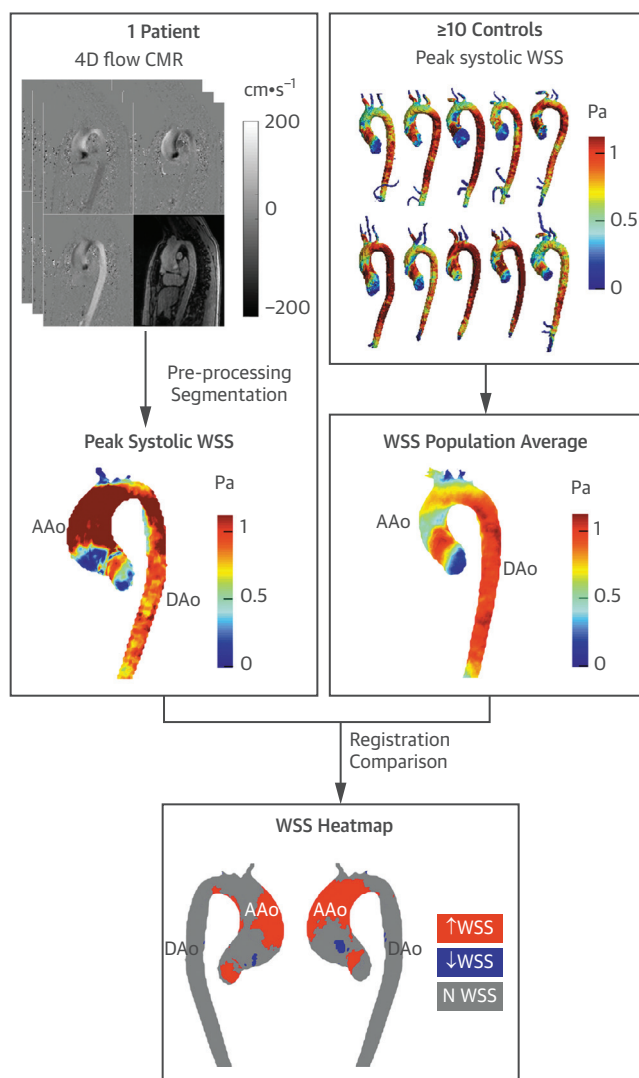
In addition, each subject underwent free-breathing, prospectively electrocardiography- and respiratory navigator-gated 4D flow CMR covering the entire thoracic aorta in sagittal oblique orientation 15 minutes-20 minutes after the administration of the gadolinium contrast agent. The scan parameters were as follows: spatial resolution =  $1.8 \text{ to } 2.7 \times 1.8 \text{ to } 2.7 \times 2.4 \text{ to } 3.5 \text{ mm}^3$ , slab coverage = 62 to 96 mm, temporal resolution = 33 milliseconds-42 milliseconds, repetition time = 4.1 milliseconds-5.3 milliseconds, echo time = 2.2 to 2.8 milliseconds, flip angle =  $7^\circ$  to  $15^\circ$ , velocity sensitivity = 150 to 300 cm/s in all 3 directions, GRAPPA (GeneRALized Autocalibrating Partial Parallel Acquisition) of 2 to 3, and a total scan time of 8 minutes-15 minutes.

**CMR DATA ANALYSIS: LEFT VENTRICULAR AND VALVE FUNCTION.** Using the SSFP short-axis stack, the left ventricular mass, end-diastolic volume, and end-systolic volume were quantified by tracing endocardial and epicardial contours, including papillary muscles in the cavity, using the Simpson method. The ejection fraction and stroke volume were calculated, and the end-diastolic and end-systole volumes were normalized to the body surface area. The aortic regurgitant fraction was estimated from the 2D phase-contrast slice at the sinotubular junction by manually segmenting the aortic lumen with background phase offsets corrected using static tissue background correction (19). Analysis was done using cvi42 (Circle) by a single observer (G.S.).

**CMR DATA ANALYSIS: AORTIC DIMENSION AND GROWTH RATES.** Aortic dimensions were measured perpendicular to the vessel centerline according to guidelines (1,18) by the same observer (G.S.) with 9 years of experience in cardiovascular CMR and blinded to the 4D flow analysis. Measurements were performed on cvi42 using multiplanar reformatting of either the 3D contrast-enhanced MRA or 3D SSFP databased on availability. Aortic dimensions at the sinus of Valsalva were quantified sinus to sinus; at other aortic locations (sinotubular junction, mid-AAo, proximal arch, midarch, proximal descending aorta, mid-descending aorta, and diaphragmatic aorta), 2 orthogonal aortic lumen diameter measurements were taken and averaged.

To decrease reliance on a single location, measurements at the sinotubular junction, mid-AAo, and proximal arch were averaged to obtain the mean AAo diameter. The AAo growth rate was calculated by

**FIGURE 1 WSS Heat Maps and Relative Area of Elevated WSS**



**(Left)** For each patient, 4D flow data (**top**) were analyzed to calculate peak systolic 3D WSS mapped onto the 3D segmentation of the aorta (**middle**). **(Right)** Peak systolic 3D aortic WSS was calculated for  $\geq 10$  healthy controls within 5 years of the target patient age to obtain a normal age- and sex-matched population average. **(Bottom)** A patient-specific WSS heat map of the patient aorta was computed relative to a map of the population average. WSS regions outside the healthy 95% CIs were classified as abnormal and mapped onto 3D visualizations of the patient-specific aorta (**red** = elevated, **blue** = reduced, **gray** = normal). 3D = 3-dimensional; 4D = 4-dimensional; AAo = ascending aorta; CMR = cardiac magnetic resonance; DAo = descending aorta; WSS = wall shear stress.

dividing the baseline versus the follow-up mean AAo diameter difference by the time interval between scans.

**CMR DATA ANALYSIS: AORTIC 4D FLOW CMR, WSS, AND WSS HEAT MAPS.** Four-dimensional flow CMR data analysis followed a previously described

**TABLE 1 Patient Baseline Characteristics (N = 72)**

Age at baseline (y)	45.3 ± 12.2
Male	50 (69)
Follow-up duration (y)	6.0 (5.5-6.7)
BSA (m <sup>2</sup> )	1.95 ± 0.21
BMI (kg/m <sup>2</sup> )	25.1 (23.4-28.0)
Heart rate (beats/min)	63 (59-72)
Hypertension	14 (19)
Beta-blockers	24 (33)
ARB	7 (10)
ACEI	7 (10)
LV at baseline (n = 71)	
EDV/BSA (mL/m <sup>2</sup> )	79.2 (64.5-94.7)
ESV/BSA (mL/m <sup>2</sup> )	30.5 (24.1-37.1)
EF (%)	62.1 ± 6.5
SV (mL)	93.7 (77.2-111.5)
Mass/BSA (g/m <sup>2</sup> )	54.7 (46.1-63.3)
Aortic regurgitant fraction (%)	6.8 (3.1-14.0)
Aortic regurgitant fraction grade (n = 71)	
None to trace	43 (61)
Mild	20 (28)
Moderate	8 (11)
Aortic stenosis grade	
None to trace	64 (89)
Mild	5 (7)
Moderate	3 (4)

Values are mean ± SD, n (%), or median (interquartile range).  
 ACEI = angiotensin-converting enzyme inhibitors; ARB = angiotensin receptor blockers; BMI = body mass index; BSA = body surface area; EDV = end-diastolic volume; EF = ejection fraction; ESV = end-systolic volume; LV = left ventricle; SV = stroke volume.

preprocessing workflow (16) with corrections for Maxwell terms, eddy currents, and velocity aliasing. Next, a 3D segmentation of the thoracic aorta distal to the aortic valve was created using a fully automated algorithm (20) and subsequently manually refined using commercial software (Mimics Innovation Suite, Materialize) if necessary. The distal end of the AAo was defined by a 2D plane placed perpendicular to the aorta lumen immediately proximal to the brachiocephalic trunk. Systolic peak velocity was calculated by automatically quantifying the maximum velocity in the AAo at peak systole as described previously (21). The degree of aortic stenosis was graded from peak velocity (mild: 2.6-2.9, moderate 3.0-4.0, and severe 4.0 m/s) (22).

Patient-specific WSS heat maps were computed relative to a WSS map of the population average for healthy age- and sex-matched controls as described previously (12,15,16,23). Briefly, after basic assumptions (ie, no flow occurring through the wall [16]), the 3D systolic WSS magnitude on the surface of the aorta was calculated at peak systole for each patient (Figure 1, left). Individual components of WSS (axial and circumferential) were not separately analyzed.

**TABLE 2 Aortic Dimensions at Baseline and Growth Rates of the Aorta**

	Aortic Dimension at Baseline (mm)	Growth Rate (mm/y)
Sinus of Valsalva	37.0 ± 4.2	0.14 ± 0.23
Sinotubular junction	32.5 ± 4.2	0.17 ± 0.24
Mid-AAo	38.2 ± 5.6	0.31 ± 0.25
Proximal arch	30.7 ± 4.0	0.25 ± 0.24
Midarch	24.4 ± 2.9	0.16 ± 0.19
Isthmus	22.1 ± 2.8	0.16 ± 0.18
Mid-DAo	21.5 ± 2.7	0.19 ± 0.19
Diaphragmatic aorta	20.1 ± 2.5	0.18 ± 0.19
Mean AAo	33.8 ± 4.1	0.24 ± 0.20

Values are mean ± SD. The mean AAo is calculated from the average of the sinotubular junction, the mid-AAo, and the proximal arch.  
 AAo = ascending aorta; Dao = descending aorta.

In addition to the regionally resolved WSS, the mean WSS and the maximum WSS (98th percentile) of the AAo and the entire aorta were calculated. To identify regions of abnormal WSS, a normal population “atlas” was generated for each patient based on the 4D flow-derived 3D systolic WSS magnitude of 10 or more healthy controls matched for age (within 5 years of patient age) and sex. For example, for a 27-year-old male patient, the WSS population average comprised 10 healthy male controls ranging from 22-32 years of age from the cohort of 136 healthy controls (Figure 1, top right and middle) (12). For each patient, a WSS heat map was generated by spatially registering the patient data to the corresponding age/sex-matched population average WSS (Figure 1, bottom). WSS regions outside the age- and sex-matched healthy control 95% CIs were classified as abnormal (11). Aortic regions of normal, depressed, and elevated WSS were mapped onto 3D visualizations of patient-specific aortas (Figure 1, bottom). The relative areas (in %) of the AAo and the entire aorta exposed to elevated WSS were quantified. The typical 4D flow analysis time including preprocessing, segmentation, and WSS calculation was 15 minutes-20 minutes.

**STATISTICAL ANALYSIS.** Baseline characteristics are provided as mean ± SD or median (interquartile range [IQR]) as appropriate. Two patient groups were defined as slower or faster aortic growth rates based on the mean AAo growth rate of the cohort (which was normally distributed). Normality was tested using the Shapiro-Wilk test. A 2-tailed Student's *t*-test or a Wilcoxon test were used to compare the 2 groups depending on normality. The Fisher exact test was used for categorical variables. The Wilcoxon signed rank test was used to compare 4D flow data between baseline and follow-up. Binary logistic regression was

performed to identify predictors of high vs low aortic growth rates. A  $P$  value  $<0.05$  was used to indicate statistical significance. Analysis was performed using SPSS 26.0 (IBM Corp).

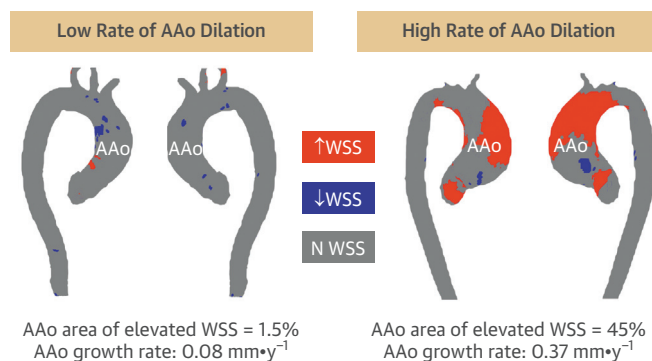
## RESULTS

The median follow-up duration was 6.0 years (IQR: 5.5 years-6.7 years). Baseline characteristics of the cohort are provided in [Table 1](#). Aortic dimensions at baseline and aortic growth rates are summarized in [Table 2](#). The AAO growth rate was  $0.24 \pm 0.20$  mm/y. Using the average AAO growth rate as a threshold, 32 of 72 patients (44%) had rates of aortic growth  $>0.24$  mm/y. Additional characteristics about the control cohort used to derive age- and sex-matched WSS population averages are provided in [Supplemental Table 1](#).

**BASELINE 4D FLOW METRICS FOR PATIENTS WITH FAST VS SLOW RATES OF AAO DILATION.** Example WSS heat maps from BAV patients with both fast ( $>0.24$  mm/y) and slow rates of AAO dilation ( $<0.24$  mm/y) are presented in [Figure 2](#), showing areas of elevated WSS in red. The patient with the higher rate of aortic dilation exhibited larger areas of elevated WSS on the heat map compared with the patient with the lower aortic growth rate.

These findings were corroborated by WSS heat map analysis across the entire cohort, as illustrated in [Figure 3](#) and [Table 3](#). At baseline, the fraction of the AAO exposed to elevated WSS was increased for patients with higher rates of aortic dilation ( $>0.24$  mm/y) compared with those with growth rates  $<0.24$  mm/y (19.9% [IQR: 10.2%-25.5%] vs 5.7% [IQR:

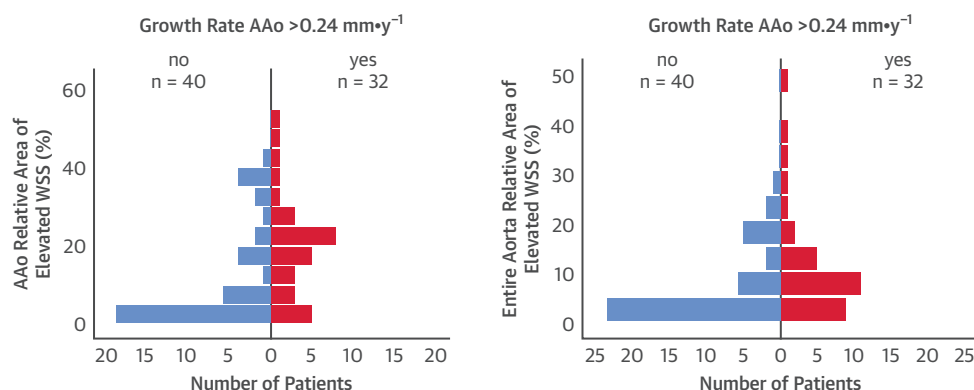
**FIGURE 2 Regionally Elevated WSS in Patients With Fast Versus Slow Rates of Aortic Dilation**



Aorta WSS heat map examples for 2 patients arranged by rate of aortic dilation (fast vs slow, defined as greater or less than 0.24 mm/y, respectively). Each panel represents right anterior and left posterior views of the patient-specific WSS heat map illustrating abnormal WSS relative to individually age- and sex-matched WSS population averages. **(Left)** BAV patient with a slow rate of aortic dilation exhibiting mostly normal aortic WSS. **(Right)** BAV patient with a high rate of aortic dilation demonstrating clearly visible areas of elevated WSS. BAV = bicuspid aortic valve; WSS = wall shear stress.

1.5%-21.3%];  $P = 0.008$ ). Similar differences were observed for the baseline area of elevated WSS over the entire thoracic aorta (9.1% [IQR: 4.8%-14.4%] vs 3.4% [IQR: 1.2%-9.7%];  $P = 0.009$ ). The peak systolic velocity was increased in patients with higher growth rates (1.74 m/s [IQR: 1.48-2.07 m/s] vs 1.48 m/s [IQR: 1.37-1.79 m/s];  $P = 0.030$ ) ([Table 3](#)). In the 58 patients with a 4D flow CMR available at follow-up, the peak systolic maximal velocity increased from 1.64 m/s (IQR: 1.43-2.01 m/s) to 1.71 m/s (IQR: 1.43-2.14 m/s;

**FIGURE 3 Incidence of Elevated WSS in Patients With High Versus Low Rates of Aortic Dilation**



Histograms of the relative area of elevated WSS in the AAO (**left**) and the entire thoracic aorta (**right**) for 40 patients with lower rates of AAO growth  $<0.24$  mm/y (**blue bars**) compared with 32 patients with higher rates of progressive AAO dilation  $>0.24$  mm/y (**red bars**). AAO = ascending aorta; WSS = wall shear stress.



**TABLE 3 Hemodynamic Differences at Baseline Between Groups With Higher Versus Lower Rates of AAO Dilation (N = 72)**

	GR Mean AAO >0.24 mm/y (n = 32)	GR Mean AAO <0.24 mm/y (n = 40)	P Value
AAo Vmax (m/s)	1.74 (1.48-2.07)	1.48 (1.37-1.79)	<b>0.030</b>
AAo mean WSS (Pa)	0.76 (0.67-0.93)	0.66 (0.62-0.82)	0.058
AAo maximum WSS (Pa)	1.59 (1.37-2.01)	1.38 (1.21-1.74)	0.055
AAo relative area of elevated WSS (%)	19.9 (10.2-25.5)	5.7 (1.5-21.3)	<b>0.008</b>
Entire aorta relative area of elevated WSS (%)	9.1 (4.8-14.4)	3.4 (1.2-9.7)	<b>0.009</b>

Values are median (interquartile range). **Bold** values indicate significant difference ( $P < 0.05$ ).  
AAo = ascending aorta; GR = growth rate; Vmax = maximum velocity; WSS = wall shear stress.

$P = 0.001$ ), whereas the mean and maximum WSS remained stable over time (0.69 Pa [IQR: 0.64 Pa-0.84 Pa] vs 0.75 Pa [IQR: 0.63 Pa-0.86 Pa];  $P = 0.607$  and 1.51 Pa [IQR: 1.26 Pa-1.87 Pa] vs 1.51 [IQR: 1.31 Pa-1.95 Pa];  $P = 0.078$ , respectively).

**PREDICTORS OF HIGH RATES OF PROGRESSIVE AAO DILATION.** Age, body surface area, body mass index, treatment with angiotensin receptor blockers and angiotensin-converting enzyme inhibitors, baseline AAO diameter, and aortic valve regurgitant fraction were not significantly associated with higher rates of AAO dilation ( $>0.24$  mm/y) (Table 4). Both treatment by beta-blockers and decreased heart rate were predictors of progressive AAO dilation  $>0.24$  mm/y (odds ratio [OR]: 3.03; 95% CI: 1.10-8.39;  $P = 0.032$ ; for 10 beats/min, OR: 0.55; 95% CI: 0.33-0.90;  $P = 0.018$ ).

Among 4D flow metrics, the percent areas of elevated WSS in the heat maps of the AAO and the entire thoracic aorta were the only predictors of higher rates of progressive AAO dilation  $>0.24$  mm/y (for 10% increase, OR: 1.51; 95% CI: 1.05-2.17;  $P = 0.026$  and OR: 1.79; 95% CI: 1.01-3.15;  $P = 0.046$ , respectively) (Table 4).

In a multivariate binary logistic regression, the percent area of elevated WSS in the AAO heat map at baseline remained significantly associated with a dilation rate  $>0.24$  mm/y after adjustment for age, sex, heart rate, and baseline AAO diameter (Model 1, Table 5) and after adjustment for valve fusion type and presence of a raphe (Model 2, Table 5).

## DISCUSSION

This study demonstrates the potential of 4D flow CMR-derived WSS heat maps as an imaging biomarker that may help identify BAV patients with higher risk of progressive aortic dilation. As shown in the Central Illustration, the fraction of the area exposed to elevated WSS on heat maps was greater in patients with faster rates of AAO dilation. On logistic

regression, the maximum and mean systolic WSS were not predictive of faster aortic growth rate at  $\geq 5$  years of follow-up, whereas the fraction of the area exposed to elevated WSS on heat maps was a predictor of faster aortic growth rate. These observations indicate the importance of relating changes in aortic WSS in the individual patient to WSS distributions of age- and sex-matched control populations—an inherent property of the WSS heat map concept.

Two theories attempt to explain progressive aortic dilation in BAV. The “primary aortopathy” hypothesis postulates a genetic origin of BAV disease based on the assumption that the matrix of the aortic wall is fragile and susceptible to dilation caused by pathological histological composition. In contrast, the “hemodynamic hypothesis” postulates that mechanotransduction forces caused by BAV-mediated abnormal blood flow can cause structural alterations to the aorta wall. This second hypothesis has been an ongoing subject of many prior studies in BAV disease. Previous studies by Hope et al (7,9) suggested that visually graded eccentric blood flow in the AAO was associated with accelerated aortic growth in patients with BAV, but the findings were limited by semiquantitative image analysis and a small cohort size. Other studies reported that hemodynamic markers such as flow displacement, higher rotational (helical) flow, and systolic outflow angle are correlated with dilation of the thoracic aorta (7,24-26). An echocardiographic study by Michelena et al (27) provided evidence that changes in aortic hemodynamics were related to aortopathy, aorta growth, and patient outcomes. A number of studies have shown that aortic WSS is a quantifiable mechanism directly associated with aortic dilation and alteration of the vessel wall architecture (8,11,17,28,29). Although various WSS-derived metrics have been proposed, such as low or oscillatory WSS (30), our work is focused on elevated WSS at peak systole. The present study provides additional evidence supporting the hemodynamic hypothesis

by documenting significant associations between elevated WSS at baseline with progressive aortic dilation in BAV at long-term follow-up. Nonetheless, both the primary aortopathy and hemodynamics hypotheses are likely to contribute; there is evidence of a genetic basis to BAV, such as a 3:1 male predominance and familial clustering (31,32). Aortic dilation, triggered by genetic wall abnormalities, could be further exacerbated by unfavorable hemodynamic conditions such as BAV-mediated outflow jets and elevated ascending aortic WSS. The stability of WSS over time in our study cohort indicates that elevated WSS may drive aortic dilation. However, long-term follow-up data in patients enrolled before any aortic dilatation are warranted to fully understand the mechanisms of aortic dilatation.

To refine our approach, WSS heat maps were designed to provide patient-specific metrics by adjusting WSS measurements for age and sex. This is relevant because aortic hemodynamics, including WSS, change substantially with aging (12,14). Of note, similar to previous studies (33,34), the peak systolic WSS remained stable over the follow-up period in our study cohort, and previous work has shown that WSS is reproducible on test-retest data (35).

Compared with a previous study with similar methodology in 13 BAV patients who received 4D flow CMR before aortic surgery, the percentage area of elevated WSS in the ascending aorta on heat maps was lower in our cohort (7% compared with 33% at the outer and 7% at the inner AAO) (15). We speculate that this is related to reduced disease severity in our patients because they did not meet surgical criteria even 5 years after baseline CMR evaluation.

Several recent studies have shown that AAO dilation is a slow gradual process. In an echocardiographic study, Della Corte et al (3) reported a median AAO growth rate ranging from 0.20 to 0.35 mm/y for BAV patients during a 4-year follow-up. In an echocardiographic study with 353 BAV patients, Detain et al (4) observed mean AAO growth rates of  $0.42 \pm 0.6$  mm/y in BAV patients based on a 3.6-year follow-up period but a large proportion (43%) with no or very minor progression of aortic dilation. Although growth rates in our study cohort were low, our observed growth rate of 0.24 mm/y is comparable with these earlier studies with similar follow-up duration (3,4). We speculate that this is related to the inclusion of patients with existing >5-year follow-up CMR data without surgery. BAV patients with aortic growth on the order of several millimeters per year would have most likely been referred for aortic surgery before the 5-year follow-up.

**TABLE 4 Univariate Binary Logistic Regression for Higher Rates of AAO Dilation (>0.24 mm/y) in BAV Patients (N = 72)**

	OR	95% CI	P Value
Age, 10 y	0.89	0.60-1.31	0.541
Heart rate, 10 beats/min	0.55	0.33-0.90	<b>0.018</b>
BSA, 0.1 m <sup>2</sup>	1.23	0.97-1.57	0.085
BMI	1.03	0.92-1.16	0.608
Hypertension, yes	0.64	0.19-2.14	0.466
Raphe, no	1.89	0.58-6.15	0.291
RN fusion, yes	1.57	0.50-4.92	0.438
Beta-blockers, yes	3.03	1.10-8.39	<b>0.032</b>
ARB, yes	0.38	0.07-2.02	0.254
ACEI, yes	0.18	0.02-1.60	0.125
AAo diameter, 5 mm	1.09	0.61-1.94	0.764
Aortic regurgitant fraction, 10%	1.28	0.83-1.97	0.258
4D flow metrics at baseline			
AAo Vmax, 0.1 m/s	1.08	0.98-1.19	0.132
AAo mean WSS, 0.1 Pa	1.37	0.92-2.04	0.124
AAo maximum WSS, 0.1 Pa	1.06	0.96-1.17	0.231
AAo relative area of elevated WSS, 10%	1.51	1.05-2.17	<b>0.026</b>
Entire aorta relative area of elevated WSS, 10%	1.79	1.01-3.15	<b>0.046</b>

Univariate binary logistic regression for higher rates of AAO dilation (>0.25 mm/y) in BAV patients (N = 72). **Bold** values indicate significant difference ( $P < 0.05$ ).

ACEI = angiotensin-converting enzyme inhibitors; ARB = angiotensin receptor blockers; BMI = body mass index; BAV = bicuspid aortic valve; BSA = body surface area; OR = odds ratio; RN = right to noncoronary; other abbreviations as in Table 3.

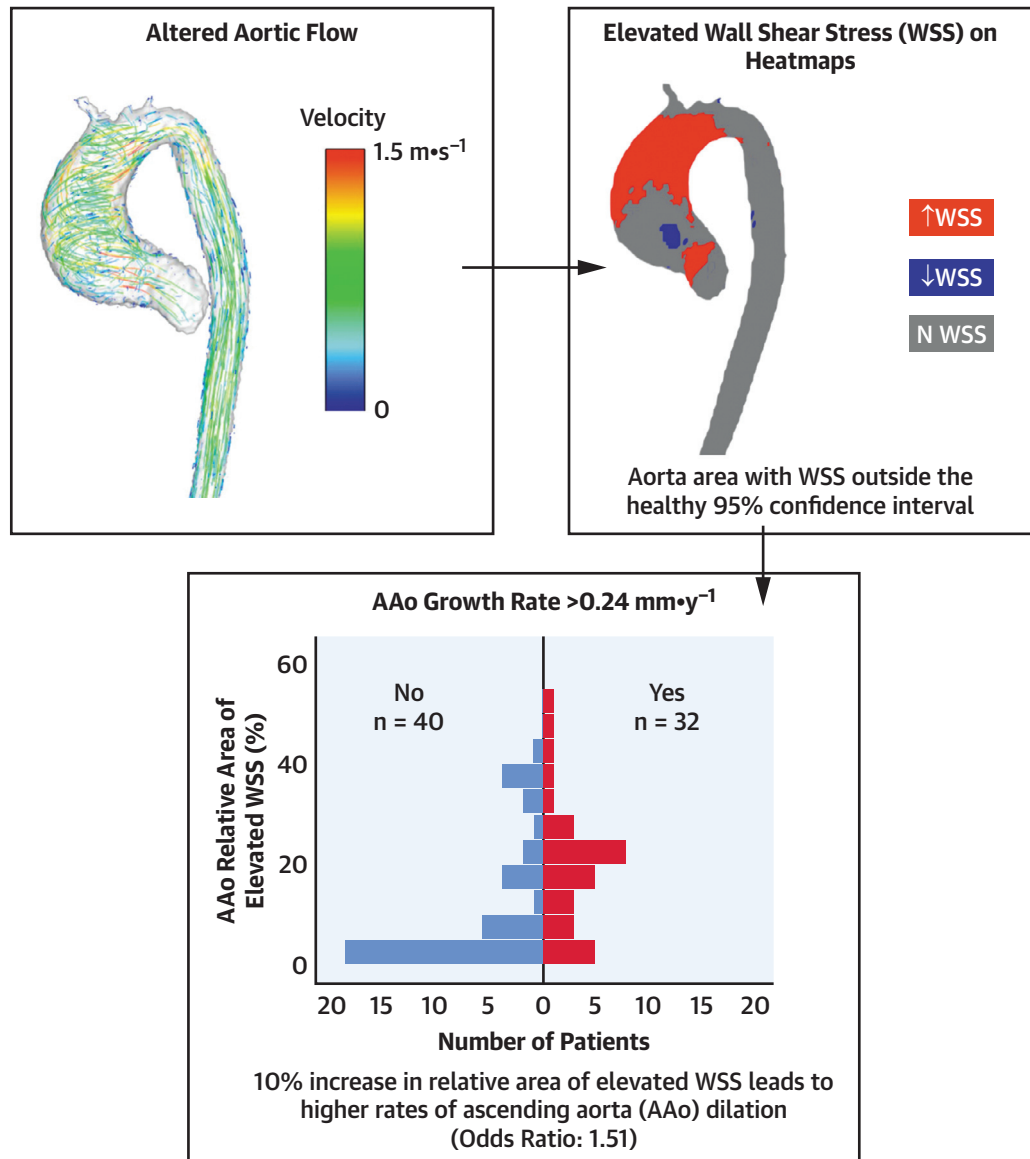
Previous studies found that WSS was influenced by aortic valve stenosis (25,28), and we observed a significant difference in AAO peak velocity between the groups with faster and slower rates of aortic growth. Although out of the scope of this study, the influence of valve dysfunction on WSS heat maps and patient outcomes (eg, referral for surgery) merits further investigation.

It is important to note that our study investigated associations of regional metrics (WSS) with a

**TABLE 5 Multivariate Binary Logistic Regression for Higher Rates of AAO Dilation (>0.24 mm/y) in BAV Patients (N = 72)**

	OR	95% CI	P Value
Model 1			
Age, 10 y	0.79	0.49-1.25	0.315
Male	1.28	0.41-4.00	0.672
Heart rate, 10 beats/min	0.53	0.31-0.91	<b>0.024</b>
AAo diameter, 5 mm	1.45	0.70-3.04	0.321
AAo relative area of elevated WSS, 10%	1.63	1.08-2.47	<b>0.019</b>
Model 2			
Age, 10 y	0.82	0.53-1.26	0.370
Male	1.40	0.46-4.22	0.552
Raphe, no	1.29	0.34-4.93	0.709
RN fusion, yes	1.83	0.50-6.75	0.365
AAo relative area of elevated WSS, 10%	1.60	1.09-2.35	<b>0.017</b>

Abbreviations as in Tables 3 and 4.

**CENTRAL ILLUSTRATION** Elevated Wall Shear Stress Secondary to Altered Aortic Flow Is Associated With Higher Rates of Progressive Dilation of the Ascending Aorta

Soulat, G. et al. J Am Coll Cardiol Img. 2021;■(■):■-■.

**(Top Left)** An example of abnormal aortic flow patterns in the ascending aorta visualized using 4D flow CMR-derived systolic 3D streamlines (higher velocities appear in red). **(Top Right):** WSS heat map from the same patient obtained using an age/sex-matched population average of healthy volunteers showing areas of abnormally elevated WSS in red (outside the 95% CI of the age/sex-matched control population). **(Bottom)** A histogram of the relative areas of elevated WSS in the ascending aorta for n = 40 patients with low rates of aortic growth  $<0.24 \text{ mm/y}$  (blue bars) compared with n = 32 patients with higher rates of progressive aortic dilation  $>0.24 \text{ mm/y}$  (red bars). 3D = 3-dimensional; 4D = 4-dimensional; CMR = cardiac magnetic resonance; WSS = wall shear stress.

measure of changes in aortic dimensions over time. Nonetheless, the WSS heat map concept used in this study was used to quantify the size of the area exposed to elevated WSS in the entire

AAo. This measure of altered AAo hemodynamics was correlated with average AAo dimensions and growth rates derived from the same aortic regions.



A methodologic limitation related to the use of 2 different MRA techniques at baseline and follow-up in some patients may have increased the variability of the measurement of aortic dimensions. However, we used different MRA techniques in only 8 of the total 72 BAV patients (11%) enrolled in our study. As a result, differences in MRA techniques may have increased the variability of aortic measurements, but we are confident that had only a minimal impact (bias) on the relationship with WSS.

A counterintuitive finding in our study was the higher risk of faster aortic growth in patients undergoing beta-blocker therapy. This should be interpreted with caution because patients were not randomized for treatment, and patients with faster aortic growth or who were otherwise considered higher risk by their physicians may have been more likely to be prescribed beta-blockers.

**STUDY LIMITATIONS.** The total number of patients enrolled in our study was small caused by the recent application of the 4D flow approach. Although this limits the ability to translate these findings to practice, it provides promising insight for future studies in larger cohorts. Similarly, a larger reference sample for WSS is needed to improve the definition of normal ranges. To our knowledge, this is the largest longitudinal study to date to investigate the predictive value of 4D flow CMR to assess risk for AAo dilation in BAV patients. However, our study may be limited by a selection bias related to the retrospective design. This may have led to the exclusion of patients with higher baseline aortic dimensions or severe aortic valve stenosis because they are more likely to have undergone surgery during the 5-year follow-up interval. In addition, studying younger patients could add valuable information on the early development of BAV aortopathy. Although the average age of our cohort was 45 (similar to previous works [3,4]), younger patients with mild BAV disease may have been excluded caused by a lack of standard of care surveillance CMR in this group. Finally, the retrospective design also makes it difficult to account for the effects of other parameters such as blood pressure or treatments. To address the potential selection bias, a future prospective study including observations at regular intervals is warranted to study aortic WSS, clinical factors, and rate of aortic growth more systematically.

## CONCLUSIONS

In BAV patients, the relative area of abnormally elevated WSS on 4D flow-derived aorta WSS heat maps was associated with faster rates of progressive AAo dilation over a greater than 5-year observation period. The detection of elevated WSS as a possible mechanism for progressive AAo dilation may help to identify BAV patients at greater risk for aortic complications. Future studies in larger cohorts are warranted to confirm these findings and to assess the diagnostic value of 4D flow-derived WSS for the management of patients with AAo dilation.

## FUNDING SUPPORT AND AUTHOR DISCLOSURES

Funding was provided by National Institutes of Health (grant nos. R01HL115828, R01HL133504, and F30HL145995). Dr Soulat received a grant support from the French College of Radiology Teachers and French Radiology Society. Additional support was provided by the Melman Bicuspid Aortic Valve Program, Bluhm Cardiovascular Institute. Dr Malaisrie has received honoraria and a research grant from Terumo Aortic. Dr McCarthy has received royalties and honoraria for speaking for Edwards Lifesciences. Dr Markl has received research support from Siemens Healthineers; a research grant and consulting fees from Circle Cardiovascular Imaging; and a research grant from Cryolife Inc. All other authors have reported that they have no relationships relevant to the contents of this paper to disclose.

**ADDRESS FOR CORRESPONDENCE:** Dr Michael Markl, Department of Radiology, Northwestern University, 737 N Michigan Avenue, Suite 1600, Chicago, Illinois 60611, USA. E-mail: [mmarkl@northwestern.edu](mailto:mmarkl@northwestern.edu).

## PERSPECTIVES

**COMPETENCY IN MEDICAL KNOWLEDGE:** The area of elevated WSS in the AAo using 4D flow can predict higher rates of aortic dilation and might help to determine which BAV patients require closer follow-up.

**TRANSLATIONAL OUTLOOK:** The findings of this study indicate a potential role of altered WSS as a mechanism of arterial wall remodeling leading to higher rates of progressive aortic dilation, thus exposing BAV patients to a greater risk for aortic complications. Future studies in larger cohorts are warranted to confirm these findings and to refine in which subtypes of BAV patients WSS heat maps might be most predictive of patient outcome.

## REFERENCES

1. Authors/Task Force Members, Erbel R, Aboyans V, et al. 2014 ESC Guidelines on the diagnosis and treatment of aortic diseases: Document covering acute and chronic aortic diseases of the thoracic and abdominal aorta of the adult. The Task Force for the Diagnosis and Treatment of Aortic Diseases of the European Society of Cardiology (ESC). *Eur Heart J*. 2014;35:2873-2926.
2. Borger MA, Fedak PWM, Stephens EH, et al. The American Association for Thoracic Surgery consensus guidelines on bicuspid aortic valve-related aortopathy: full online-only version. *J Thorac Cardiovasc Surg*. 2018;156:e41-e74.
3. Della Corte A, Bancone C, Buonocore M, et al. Pattern of ascending aortic dimensions predicts the growth rate of the aorta in patients with bicuspid aortic valve. *J Am Coll Cardiol Img*. 2013;6:1301-1310.
4. Detaint D, Michelena HI, Nkomo VT, Vahanian A, Jondeau G, Sarano ME. Aortic dilatation patterns and rates in adults with bicuspid aortic valves: a comparative study with Marfan syndrome and degenerative aortopathy. *Heart*. 2014;100:126-134.
5. Nishimura RA, Otto CM, Bonow RO, et al. 2014 AHA/ACC guideline for the management of patients with valvular heart disease. *J Am Coll Cardiol*. 2014;63:e57-e185.
6. Hiratzka LF, Creager MA, Isselbacher EM, et al. Surgery for aortic dilatation in patients with bicuspid aortic valves. *J Am Coll Cardiol*. 2016;67:724-731.
7. Hope MD, Wrenn J, Sigovan M, Foster E, Tseng EE, Saloner D. Imaging biomarkers of aortic disease: increased growth rates with eccentric systolic flow. *J Am Coll Cardiol*. 2012;60:356-357.
8. Barker AJ, Markl M, Burk J, et al. Bicuspid aortic valve is associated with altered wall shear stress in the ascending aorta. *Circ Cardiovasc Imaging*. 2012;5:457-466.
9. Hope MD, Sigovan M, Wrenn SJ, Saloner D, Dyverfeldt P. MRI hemodynamic markers of progressive bicuspid aortic valve-related aortic disease: MRI aortic hemodynamic markers. *J Magn Reson Imaging*. 2014;40:140-145.
10. van der Palen RL, Roest AA, van den Boogaard PJ, de Roos A, Blom NA, Westenberg JJ. Scan-rescan reproducibility of segmental aortic wall shear stress as assessed by phase-specific segmentation with 4D flow MRI in healthy volunteers. *MAGMA*. 2018;31:653-663.
11. Guzzardi DG, Barker AJ, van Ooij P, et al. Valve-related hemodynamics mediate human bicuspid aortopathy. *J Am Coll Cardiol*. 2015;66:892-900.
12. van Ooij P, Garcia J, Potters WV, et al. Age-related changes in aortic 3D blood flow velocities and wall shear stress: implications for the identification of altered hemodynamics in patients with aortic valve disease: age-related changes in 3D velocity and WSS. *J Magn Reson Imaging*. 2016;43:1239-1249.
13. Callaghan FM, Bannon P, Barin E, et al. Age-related changes of shape and flow dynamics in healthy adult aortas: a 4D flow MRI study. *J Magn Reson Imaging*. 2019;49:90-100.
14. Scott MB, Huh H, van Ooij P, et al. Impact of age, sex, and global function on normal aortic hemodynamics. *Magn Reson Med*. 2020;84(4):2088-2102.
15. van Ooij P, Potters WV, Collins J, et al. Characterization of abnormal wall shear stress using 4D flow MRI in human bicuspid aortopathy. *Ann Biomed Eng*. 2015;43:1385-1397.
16. van Ooij P, Potters WV, Nederveen AJ, et al. A methodology to detect abnormal relative wall shear stress on the full surface of the thoracic aorta using four-dimensional flow MRI. *Magn Reson Med*. 2015;73:1216-1227.
17. Bollache E, Guzzardi DG, Sattari S, et al. Aortic valve-mediated wall shear stress is heterogeneous and predicts regional aortic elastic fiber thinning in bicuspid aortic valve-associated aortopathy. *J Thorac Cardiovasc Surg*. 2018;156:2112-2120.e2.
18. Schulz-Menger J, Bluemke DA, Bremerich J, et al. Standardized image interpretation and post-processing in cardiovascular magnetic resonance - 2020 update: Society for Cardiovascular Magnetic Resonance (SCMR): Board of Trustees Task Force on Standardized Post-Processing. *J Cardiovasc Magn Reson*. 2020;22:19.
19. Zoghbi WA, Adams D, Bonow RO, et al. Recommendations for noninvasive evaluation of native valvular regurgitation. *J Am Soc Echocardiogr*. 2017;30:303-371.
20. Berhane H, Scott M, Elbaz M, et al. Fully automated 3D aortic segmentation of 4D flow MRI for hemodynamic analysis using deep learning. *Magn Reson Med*. 2020;84(4):2204-2218.
21. Rose MJ, Jarvis K, Chowdhary V, et al. Efficient method for volumetric assessment of peak blood flow velocity using 4D flow MRI. *J Magn Reson Imaging*. 2016;44:1673-1682.
22. Baumgartner H, Hung J, Bermejo J, et al. Recommendations on the echocardiographic assessment of aortic valve stenosis: a focused update from the European Association of Cardiovascular Imaging and the American Society of Echocardiography. *J Am Soc Echocardiogr*. 2017;30:372-392.
23. Potters WV, van Ooij P, Marquering H, vanBavel E, Nederveen AJ. Volumetric arterial wall shear stress calculation based on cine phase contrast MRI: volumetric wall shear stress calculation. *J Magn Reson Imaging*. 2015;41:505-516.
24. Bissell MM, Hess AT, Biasioli L, et al. Aortic dilation in bicuspid aortic valve disease: flow pattern is a major contributor and differs with valve fusion type. *Circ Cardiovasc Imaging*. 2013;6:499-507.
25. Shan Y, Li J, Wang Y, et al. Aortic shear stress in patients with bicuspid aortic valve with stenosis and insufficiency. *J Thorac Cardiovasc Surg*. 2017;153:1263-1272.e1.
26. Rodriguez-Palomares JF, Dux-Santoy L, Guala A, et al. Aortic flow patterns and wall shear stress maps by 4D-flow cardiovascular magnetic resonance in the assessment of aortic dilatation in bicuspid aortic valve disease. *J Cardiovasc Magn Reson*. 2018;20:28.
27. Michelena HI, Desjardins VA, Avierinos J-F, et al. Natural history of asymptomatic patients with normally functioning or minimally dysfunctional bicuspid aortic valve in the community. *Circulation*. 2008;117:2776-2784.
28. van Ooij P, Markl M, Collins JD, et al. Aortic valve stenosis alters expression of regional aortic wall shear stress: new insights from a 4-dimensional flow magnetic resonance imaging study of 571 subjects. *J Am Heart Assoc*. 2017;6(9):e005959.
29. Mahadevia R, Barker AJ, Schnell S, et al. Bicuspid aortic cusp fusion morphology alters aortic three-dimensional outflow patterns, wall shear stress, and expression of aortopathy. *Circulation*. 2014;129:673-682.
30. Dux-Santoy L, Guala A, Sotelo J, et al. Low and oscillatory wall shear stress is not related to aortic dilation in patients with bicuspid aortic valve: a time-resolved 3-dimensional phase-contrast magnetic resonance imaging study. *Arterioscler Thromb Vasc Biol*. 2020;40:e10-e20.
31. Cripe L, Andelfinger G, Martin LJ, Shooner K, Benson DW. Bicuspid aortic valve is heritable. *J Am Coll Cardiol*. 2004;44:138-143.
32. Huntington K, Hunter AG, Chan KL. A prospective study to assess the frequency of familial clustering of congenital bicuspid aortic valve. *J Am Coll Cardiol*. 1997;30:1809-1812.
33. Rose MJ, Rigsby CK, Berhane H, et al. 4-D flow MRI aortic 3-D hemodynamics and wall shear stress remain stable over short-term follow-up in pediatric and young adult patients with bicuspid aortic valve. *Pediatr Radiol*. 2019;49:57-67.
34. Rahman O, Scott M, Bollache E, et al. Interval changes in aortic peak velocity and wall shear stress in patients with bicuspid aortic valve disease. *Int J Cardiovasc Imaging*. 2019;35:1925-1934.
35. van Ooij P, Powell AL, Potters WV, Carr JC, Markl M, Barker AJ. Reproducibility and interobserver variability of systolic blood flow velocity and 3D wall shear stress derived from 4D flow MRI in the healthy aorta. *J Magn Reson Imaging*. 2016;43:236-248.

**KEY WORDS** 4-dimensional flow, aortic dilation, bicuspid aortic valve, wall shear stress

**APPENDIX** For a supplemental table, please see the online version of this paper.